Xi Engineering Consultants

East Anglia One Piling Noise

Underwater Noise

Technical Report presented to: SRSL

26/04/2021
Document number: SRSL-801-TechReport-v05

Xi Engineering Consultants, CodeBase, Argyle House, 3 Lady Lawson Street, Edinburgh, EH3 9DR, United Kingdom.
T: +44 (0)131 290 2250, xiengineering.com, Company no. SC386913

Document Summary

Xi Engineering (Xi) have issued SRSL tables detailing:

- Range to PTS and TTS from piling noise and ADD mitigation noise
- One second averaged SEL at sensor positions and noise source location used for harbour porpoise population impact modelling (un-weighted and porpoise frequency-weighted)
- 24-hour SEL_{CUM} at sensor positions (porpoise frequency weighted)

This document details methods by which these tables were produced and includes a brief summary of results.

Action	Name	Date	Version	Amendment
Originator	B. Marmo	13/8/2020	V1	Issue
Checked by	K. Cobry	19/8/2020	V2	Minor edits
Checked by	B. Marmo	20/8/2020	V3	Minor edits
Checked by	B. Marmo	04/9/2020	V4	Minor edits
Checked by		26/4/2021	V5	Minor edits

Matters relating to this document should be directed to:	
Dr Brett Marmo	E: brettmarmo@xiengineering.com
Technical Director	T: 0131 290 2249
Rebecca Horton	E: rebeccahorton@xiengineering.com
Operations Director	T: +44 131 290 2251
Principal contacts at client's organisation	
Nienke van Geel	E: Nienke.vanGeel@sams.ac.uk
	T: 01631 559 492
Chris Allen	E: Christopher.Allen@srsl.com
	T: 01631 559 391

Contents

1. Introduction

Acoustic full bandwidth (FBW) data related to the installation of the East Anglia One offshore wind farm were collected between 25th April 2018 and 30th January 2019, with pre- and post-construction data spanning from 17th February 2018 to the 16th June 2019. Nine monitoring periods were carried out, referred to as Legs, during which up to 6 sensors (RTSYS EA_SDA14) were deployed. The sensors were deployed up to ~35 km from East Anglia One. These data include noise related to impact piling of wind turbine foundations and Acoustic Deterrent Devices (ADD) used to discourage marine mammals from remaining in, or approaching regions where pile driving is about to commence. Up to 12 C-PODs were also deployed and their data used to infer the presence of harbour porpoises in the region.

The acoustic FBW data are used here to calibrate models of underwater noise propagation. These models are then used to simulate the three-dimensional sound field produced by pile and ADD activity. The sound fields are used to determine the distance from the wind turbine installation at which there is risk of permanent threshold shift (PTS) and temporary threshold shift (TTS) to the hearing of harbour porpoises. The sound fields are also used to calculate the sound exposure level (SEL) at the sensor locations averaged to one second and the cumulative SEL over a calendar day (SEL_{CUM}). The sound field and tables can be compared to contemporaneous harbour porpoise population to help determine the acoustic impact on these marine mammals.

2. Method

2.1. Modelling approach

There are several different techniques for modelling the propagation of underwater noise. The selection of methodology is dependent on the frequency of the noise being modelled. The frequency range of interest from 25 Hz and 63 kHz is very large and required more than one method to provide a robust solution. At low frequencies, the parabolic code RAMSGeo (from the open-source AcTUP suite of codes) was used. RAMSGeo becomes numerically inefficient as frequency increases, and eventually non-viable. Instead, a ray tracing code using the commercially available software package COMSOL Multiphysics was used at high frequencies. The modelling approach transitioned from RAMSGeo to ray tracing at 3 kHz. A sensitivity analysis was conducted to ensure that results were not dependent on the frequency at which the modelling approach changed, with transition frequencies between 2 and 5 kHz giving similar results.

In both modelling approaches, the bathymetry, seabed type and sound attenuation in sea water were considered. The RAMSGeo formulation includes parameters relating to seabed characteristics reflecting the complex interaction between the water column and seabed at low frequency, while the seabed was modelled as an impedance boundary in the ray tracing model.

2.2. Geometry

The bathymetry was based on data downloaded from the Admiralty Marine Data Portal (see Appendix A). Figure 1 shows the bathymetry in the modelled region around the wind farm and include the positions of sensors during Leg 9. For numerical efficiency, transmission loss was modelled in two-dimensional vertical sections radiating the noise source. This approach assumes no lateral variation in transmission loss; this assumption is reasonable in

this region where lateral variations in bathymetry are minor (as opposed to an estuarine environment where a three-dimensional approach would be more appropriate).

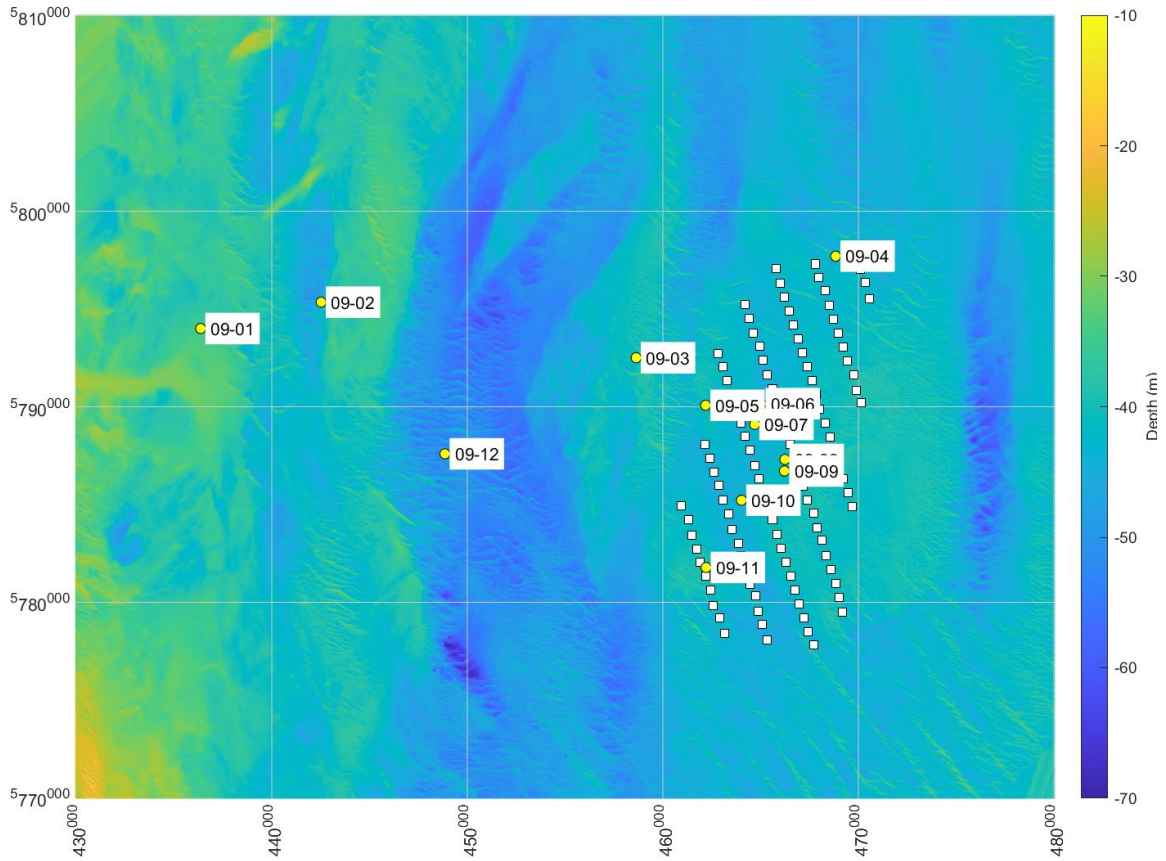

Figure 1 Bathymetry around the East Anglia One wind farm. White squares show the positions of wind turbine foundations. The yellow circles are the sensor sites during Leg 9; the second number is the location indicator (i.e. 09-01 is Leg 9 Location 1). The bathymetric map is based on data from the Admiralty Marine Data Portal. Eastings and Northings are in meters.

2.3. Material properties

The properties of the seawater and seabed sediment modelled are listed in Table 1. The attenuation coefficient of the water was modelled as being frequency dependent (Figure 1) based on the method of Ainslie & McColm (1998) using the properties listed in Table 1. The seabed is modelled as consisting of sandy sediment; its impedance condition is based on a sediment density of 2040 kg/m^3 and speed of sound of 1720 m/s (LeBlanc, Mayer, Rufino, Schock, & King, 1992).

In shallow water, the water and seabed can form a waveguide that prohibits the propagation of low frequency noise (Urick, 1983). For the given speed of sound in water and the seabed (Table 1), frequencies below 40 Hz cannot propagate.

		Sea water	Seabed sediment
Speed of sound	m/s	1500	2040
Density	kg/m^3	1026	1720
Temperature	°C	15	-
Salinity	-	35	-
pH	-	8	-

Table 1 Properties of water and the seabed used in the models. Temperature, salinity and pH were used to determine the acoustic absorption of sea water following the method of Ainslie & McColm (1998).

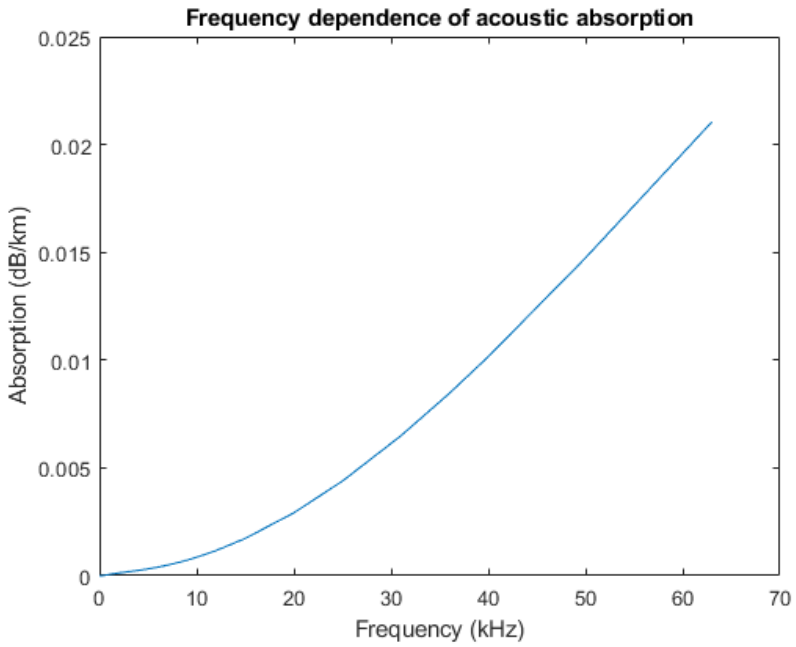

Figure 2 Attenuation of noise by sea water based on the model of Ainslie & McColm (1998).

2.4. Calibration data

Three datasets were selected by SRSL to calibrate the underwater noise models. These datasets had recordings of pilings at single sites and were selected based on:

- Having continuous contemporaneous recordings from all six sensors.

- The recordings having not been adulterated by events that are not related to piling noise, such as surface vessel noise or detonations of unexploded ordinance.
- The closest sensor being at sufficient distance from the piling event such that the acoustic signal did not exceed the sensitivity of the hydrophone (i.e. the signal did not 'clip')
- The recording included a start-up and cessation of piling to allow synchronisation of acoustic signals recorded at different sensors to account for different arrival times.

Based on these criteria, piling at wind turbines D03, C03 and E25 were selected with details listed in Table 2. All three piling events took place during Leg 5. The distances of each sensor from the piling events are listed in Table 3.

The recordings at each sensor were post-processed by SRSL and issued to Xi as one second peak sound pressure level (SPL; in dB re 1 μPa) in one-third octave bands (TOB) in a series of Excel spreadsheets on the 9th April 2020. The data were time shifted to account for different arrival times. Given that the range of each sensor from the noise source was known, the data were time shifted by assuming that the speed of sound was 1500 m/s; minor adjustments were made by visual examination of the arrival of the initial hammer blows following a cessation of pile driving. These data were used to calibrate the model. Audio .wav files were also issued to Xi, and these were visually inspected to check and help interpret the spreadsheets containing one-second peak SPL.

The models were calibrated by calculating the source levels of piling events in one third octave bands. Transmission losses were modelled for vertical sections between piling source and sensor. Source levels (in dB re 1 μPa^2sm^2 at 1 m) were then derived for each one third octave band by determining the best fit for the change of peak SPL with range from source using the coefficient of determination (i.e. R^2 of the modelled distribution compared to recorded distribution) (Figure 3).

Wind turbine	Pin	Max hammer energy (kJ)	Start of recording	End of recording
D03	C	643	24/07/2018 21:14	24/07/2018 21:25
C03	B	737	13/07/2018 23:27	13/07/2018 23:37
E25	C	617	22/07/2018 9:43	22/07/2018 9:55

Table 2 Details of piling events used to calibrate the models. Pin refers to which pin foundation was being piled during the recording period.

Sensor	Range (km)		
	Piling location		
	D03	C03	E25
05_01	35.90	34.24	29.91
05_03	16.71	15.81	8.22
05_05	12.47	11.77	7.02
05_06	11.33	11.08	5.67
05_07	10.42	10.05	6.84
05_12	21.77	20.08	19.09

Table 3 Distance between each sensor and the piling events used to calibrate the model.

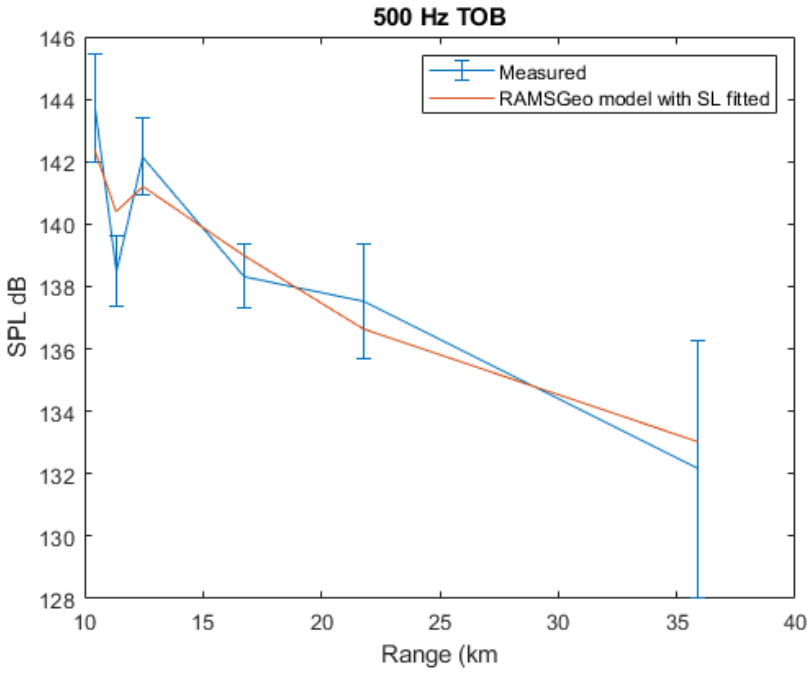

Figure 3 Example of fitting process by which the models were calibrated. This example is the 500 Hz one third octave band from piling at D03. The transmission loss profile was modelled using RAMSGeo and fitted by adjusting the source level and minimising the R^2 value.

2.5. Calculation of TTS and PTS for all events

To inform SRSL's assessment of the risk of permanent threshold shift (PTS) and temporary threshold shift (TTS) to the harbour porpoise population in the region, the cumulative sound exposure level (SEL_{CUM}) over a 24-hour period was modelled for each day with piling activity including noise from the ADD mitigation systems. The source level (SL) associated with each piling event was calculated by scaling the source levels derived in the calibration step by the hammer energy used:

$$SL = SL_{REF} + 10log_{10}\left({}^{E}/_{E_{REF}}\right)$$

where E is the hammer energy, SL_{REF} is the source level of the reference event derived in the calibration (see above), and E_{REF} is the piling energy used during the reference event.

A three-dimensional sound field for each one third octave band was modelled for each piling event by placing the noise source with appropriate source level (SL) for the given event at its correct geometric position and using the simulated transmission loss profiles to derive one-second averaged SEL throughout the model space. The sound fields were weighted for the hearing curves of harbour porpoises following the approach of Southall, et al. (2019) for cetaceans at very high frequency and the equivalent NOAA approach:

$$W_{(f)} = C + \log_{10}\left\{\frac{(f/f_1)^{2a}}{[1+(f/f_1)^2]^a[1+(f/f_2)^2]^b}\right\}$$

where f is the frequency in kHz and the constants for each mammal group are listed in **Error! Reference source not found.**.

Group	f_1	f_2	a	b	K	C
VHF (Southall et al., 2019)	12	140	1.8	2	152	1.36

Table 4 Constants used for the weighting function related to the hearing of harbour porpoises. NOAA classes use a mathematically identical approach.

The sound field weights for porpoises were used to calculate the cumulative impact over a 24-hour period. The SEL_{CUM} was calculated based on the duration of each piling event:

$$SEL_{CUM} = SEL + 10log_{10}(t)$$

where t is the duration of the event in seconds. A hammer rate of 0.66 per second was used in the SEL calculation. The hammer rate was based on inspection of audio recordings. When more than one piling event occurred on the same calendar day, the SEL_{CUM} was taken as the energy sum of all the events in the 24 hour period. The piling schedules issued in

documents *Final WTG Piling Schedule_20200713.xlsx* and *Final OFSS Piling Schedule_20200713.xlsx* (issued to Xi on the 13th July 2020), were used to obtain the piling locations, timings and durations.

The impact of ADD mitigation was included in the SEL_{CUM}. Based on the *document LOFITECH ADD info summary.doc*, the source level of the ADD was 191 dB with a frequency of 10-20 kHz and an average duty cycle of 0.12. To simplify the model, all acoustic energy produced by the ADD was assumed to be in the 16 kHz one third octave band. The SEL from ADD was modelled using a similar approach to piling noise, whereby the source was placed at the appropriate geographic position and transmission loss (in this case at 16 kHz) was used to determine the SEL at any given point. The weighting curve for harbour porpoises was applied to the SEL at 16 kHz. The SEL_{CUM} was then based on the duration that the ADD was active, in seconds, multiplied by the duty cycle. SEL_{CUM} produced by the ADD output was added to the piling noise using an energy sum, resulting in an overall 24-hour exposure level. The ADD schedules issued in documents *Final WTG ADD Schedule_20200713.xlsx* and *Final OFSS ADD Schedule_20200713.xlsx* (issued to Xi on the 13th July 2020), were used to obtain the ADD locations, timings and durations.

The range at which there is risk of TTS and PTS was then assessed by determining the maximum range at which the SEL_{CUM} for a 24-hour period exceeded the threshold for harbour porpoises. Following the approach of both Southall et al. (2019) and the NOAA guidance, these levels are 153 dB for TTS and 173 dB for PTS.

3. Results

3.1. Source level

Recordings of piling activity at D03, C03 and E25 were used to determine appropriate source level values. Spectrograms were used to assess frequencies at which piling noise was discernible above the ambient noise, and thereby determine the range of frequencies for which recordings could be used to determine source level (Figure 4). Based on visual inspection of the available data, it is reasonable to assess the source level up to frequencies of 12.5 kHz for D03, 10 kHz for C03 and 16 kHz for E25.

The source levels derived by fitting data recorded during the piling of wind turbines D03, C03 and E25 are shown in Figure 5 to Figure 7 respectively. The topology of the three derived source level spectra are generally consistent with highest level recorded in the low frequency bands, between 100 and 200 Hz. The source levels tend to decrease at frequencies above 200 Hz, and they decrease rapidly above 3.1 kHz.

The highest source levels are at piling C03 (hammer energy of 737 kJ), with a peak of 208.7 dB in the 100 Hz band. The highest level recorded from D03 (673 kJ) was 207.0 dB in the 160 Hz band, with significant levels also in the 100 Hz band (206.0 dB). The highest levels from piling E25 (617 kJ) were 205 dB in the 125 Hz band.

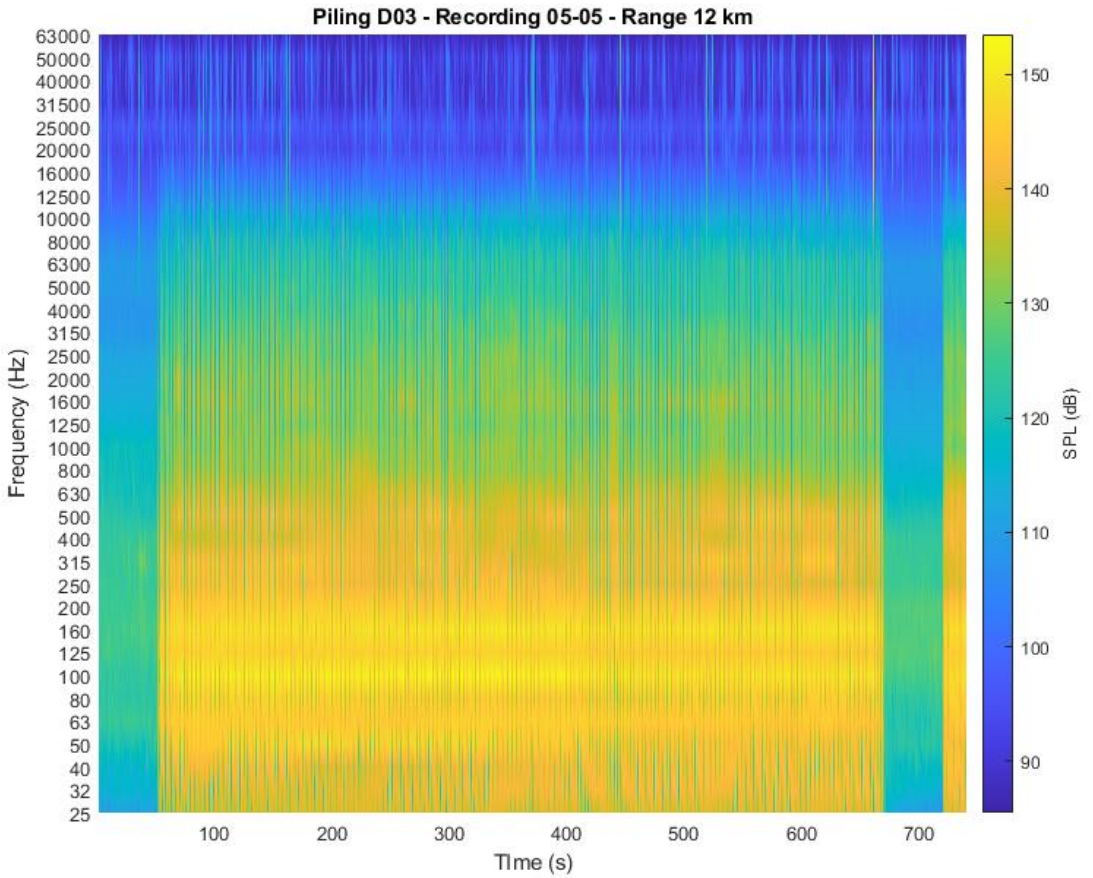

Figure 4 Example spectrogram recorded at location 5 during Leg 5 while piling at D03. The piling occurred between 50 seconds and 680 seconds, then ceased until 715 seconds before recommencing. Noise related to piling is discernible up to ~ 12.5 kHz; at higher frequencies it is not possible to discern piling noise from background noise.

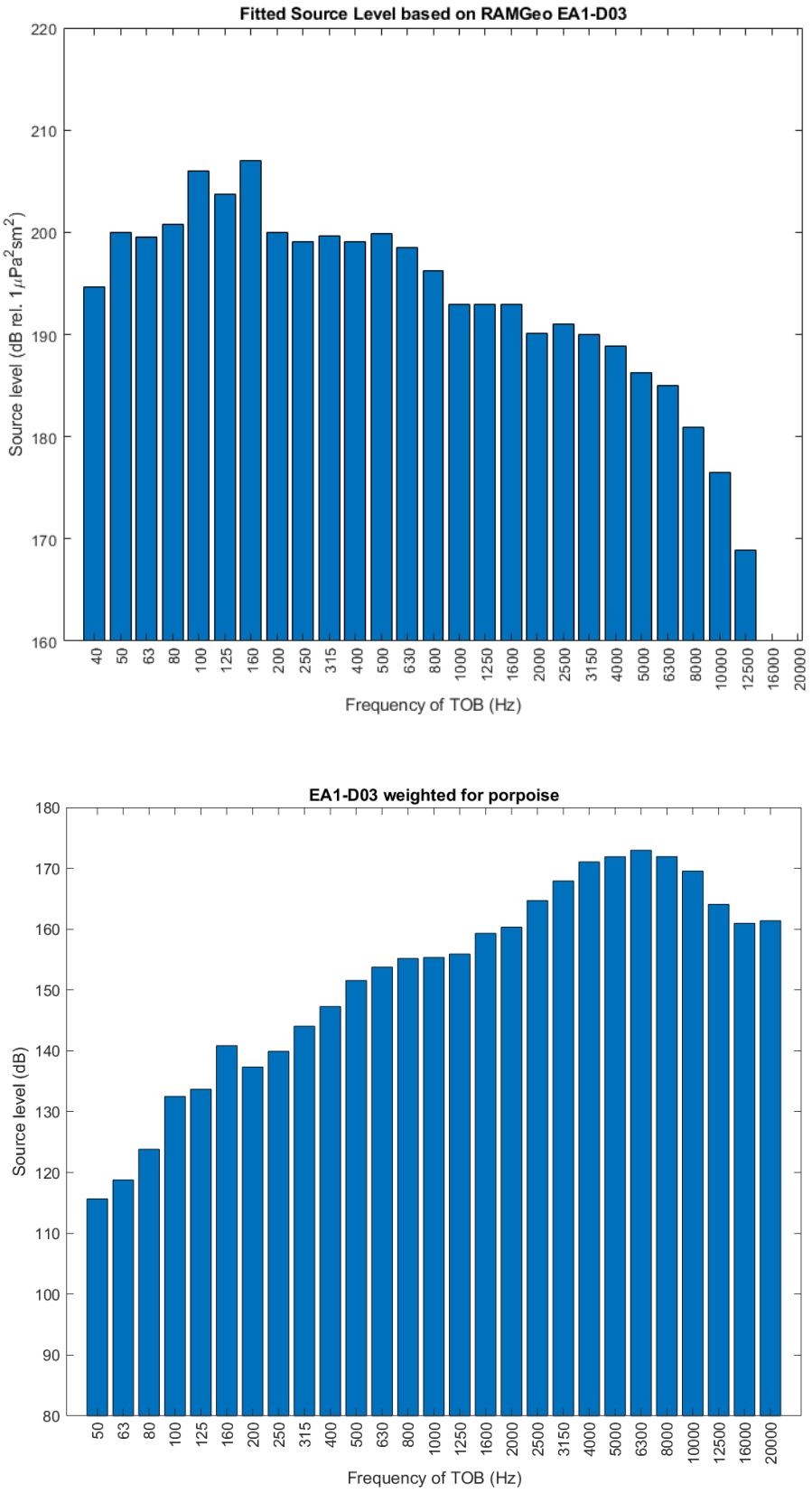

Figure 5 Source level for piling at D03 with a hammer energy of 643 kJ derived from measured data fitted with transmission loss profiles; unweighted (top) and porpoise frequency-weighted (bottom).

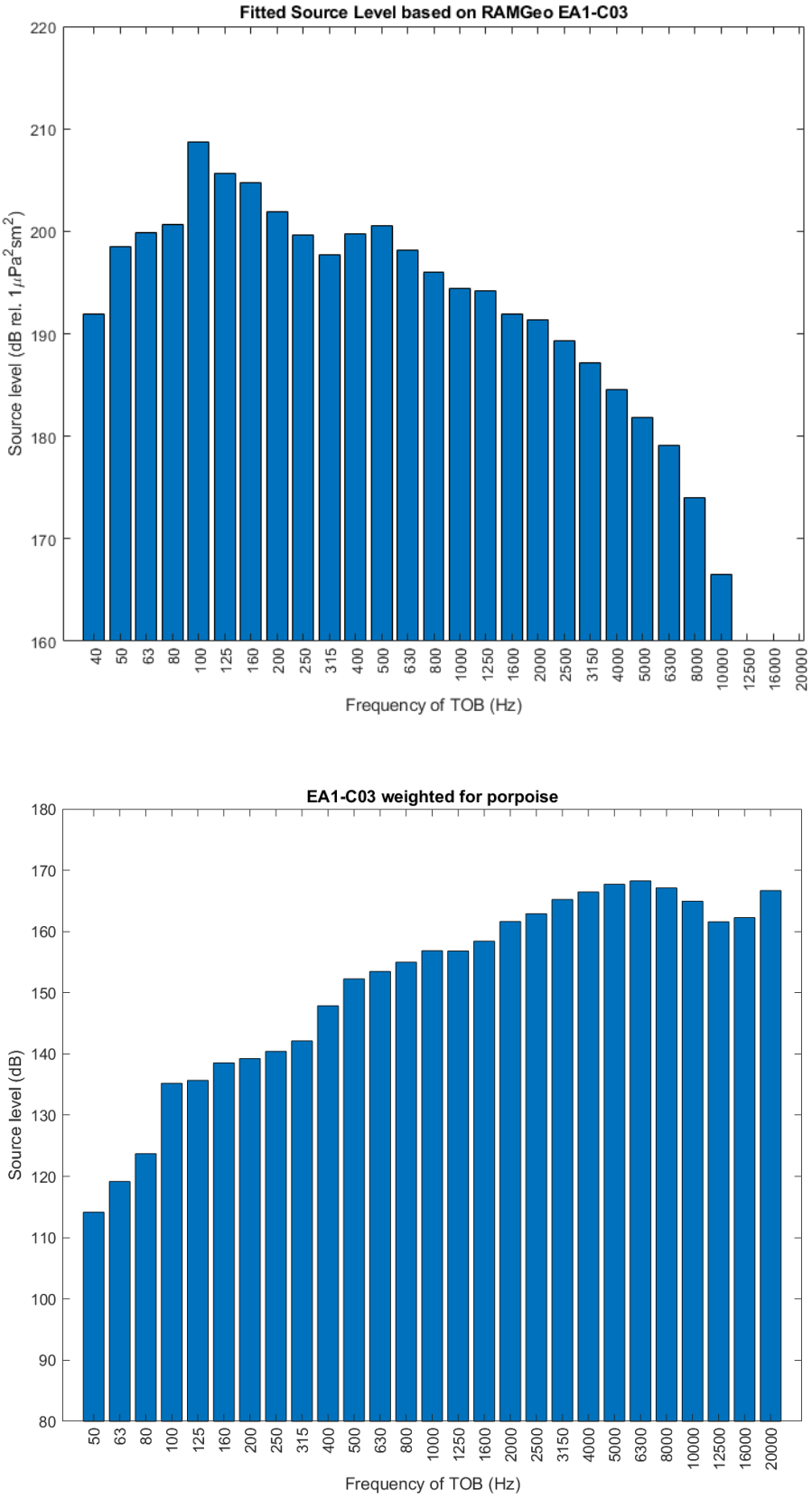

Figure 6 Source level for piling at C03 with a hammer energy of 737 kJ derived from measured data fitted with transmission loss profiles; unweighted (top) and porpoise frequency-weighted (bottom).

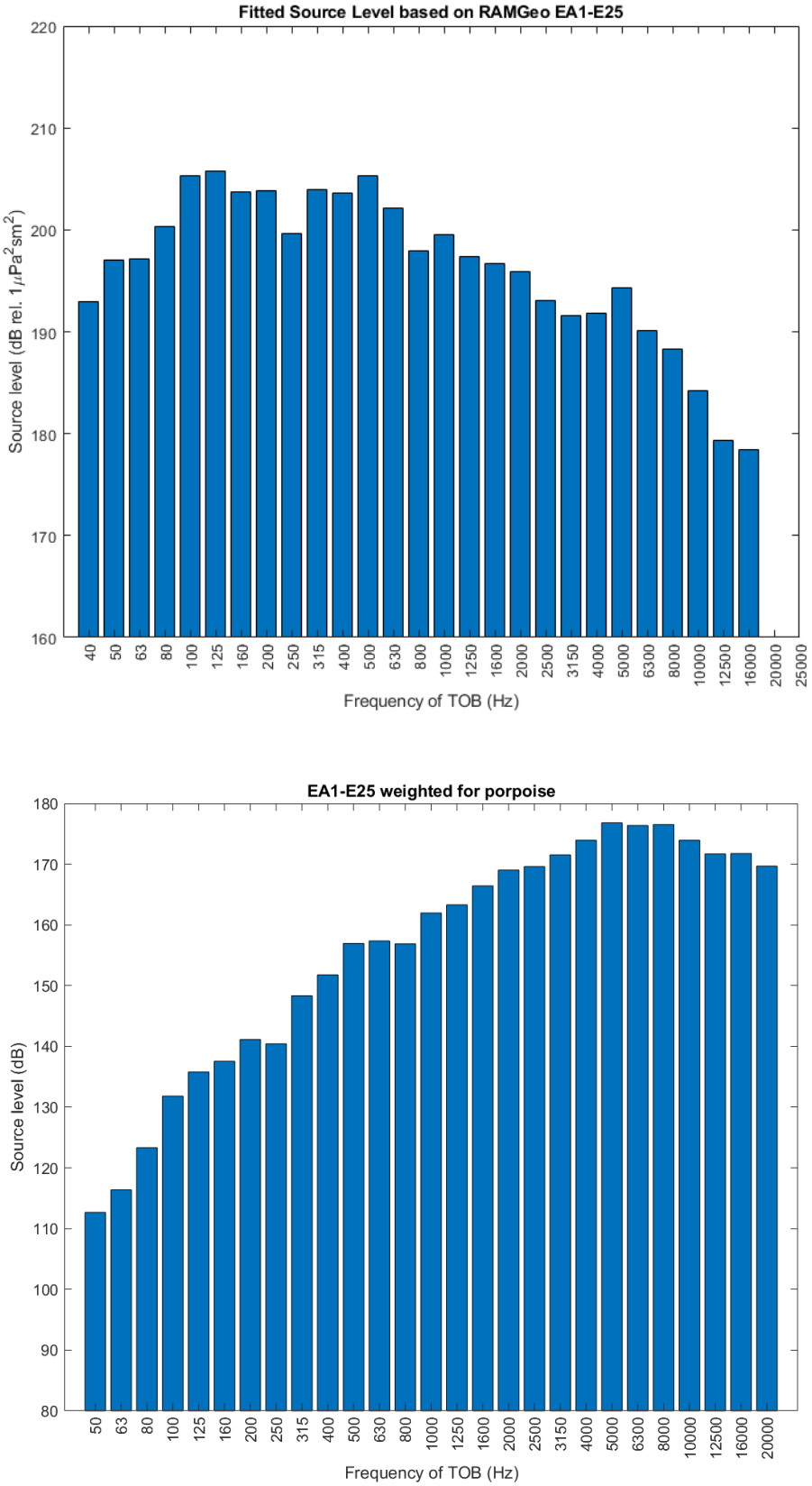

Figure 7 Source level for piling at E25 with a hammer energy of 617 kJ derived from measured data fitted with transmission loss profiles; unweighted (top) and porpoise frequency-weighted (bottom).

3.2. Range to PTS and TTS

The calculated 24-hour SEL_{CUM} were used to determine the range at which there is risk of PTS and TTS for porpoises for each day with piling activity. Results have been issued in the table *Daily 24 hour SEL 07.xlsx*. This table includes location of the source as a grid reference and the range from that reference at which there is risk of PTS and TTS. On days when activity occurs in more than one location within a calendar day, separate PTS and TTS ranges have been included for each site. Examples of piling in multiple locations in a single calendar day are shown in Figure 8 and Figure 9.

Generally, the range to PPT and TTS increase with the duration of piling activity. The median range to PTS for each day when piling occurred at East Anglia One was 600 m with a maximum of 880 m (Table 5). The median range to TTS for each day when piling occurred at East Anglia One was 5.5 km with a maximum of 8.6 km (Table 5).

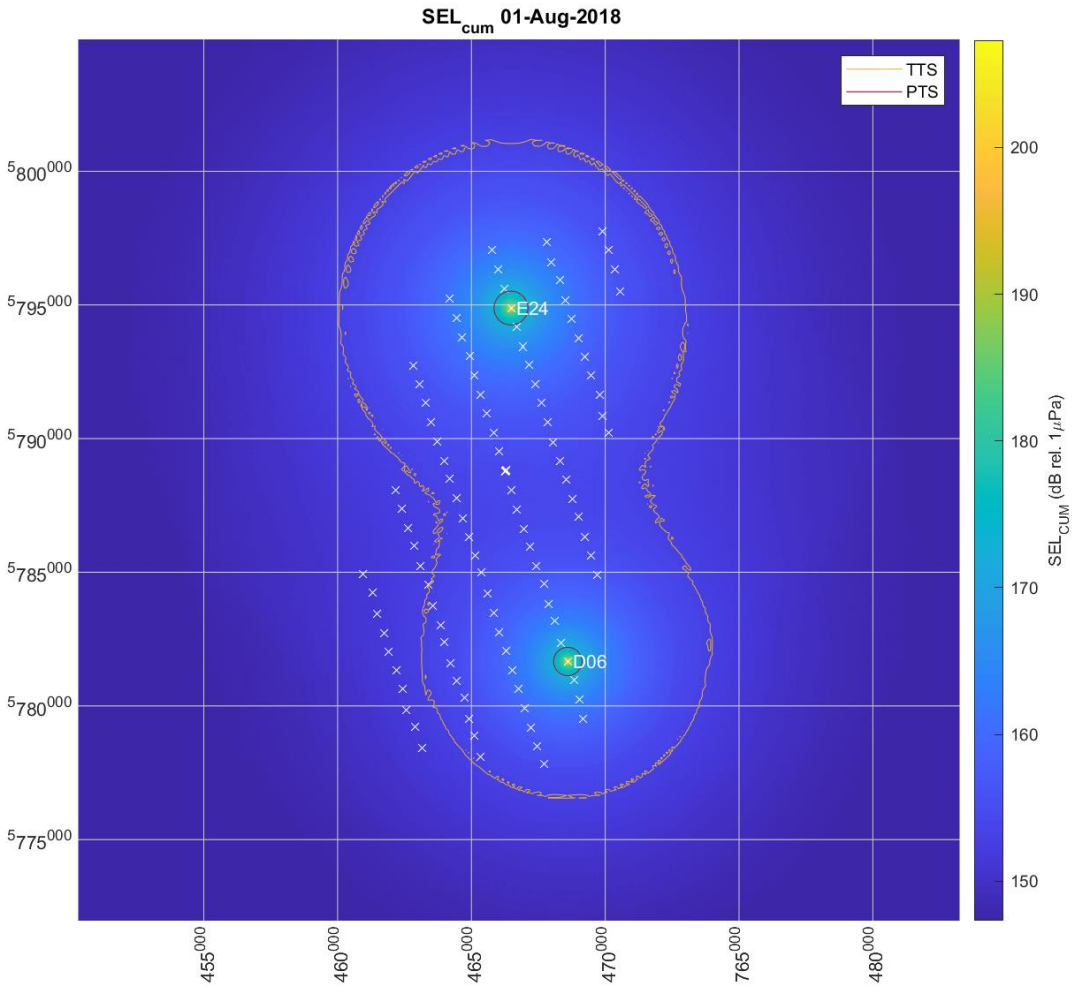

Figure 8 SEL_{CUM} for the calendar day 1st August 2020 when piling and ADD occurred at D05 and E24. SEL_{CUM} is calculated between 40 Hz and 16 kHz. Eastings and Northings are in meters.

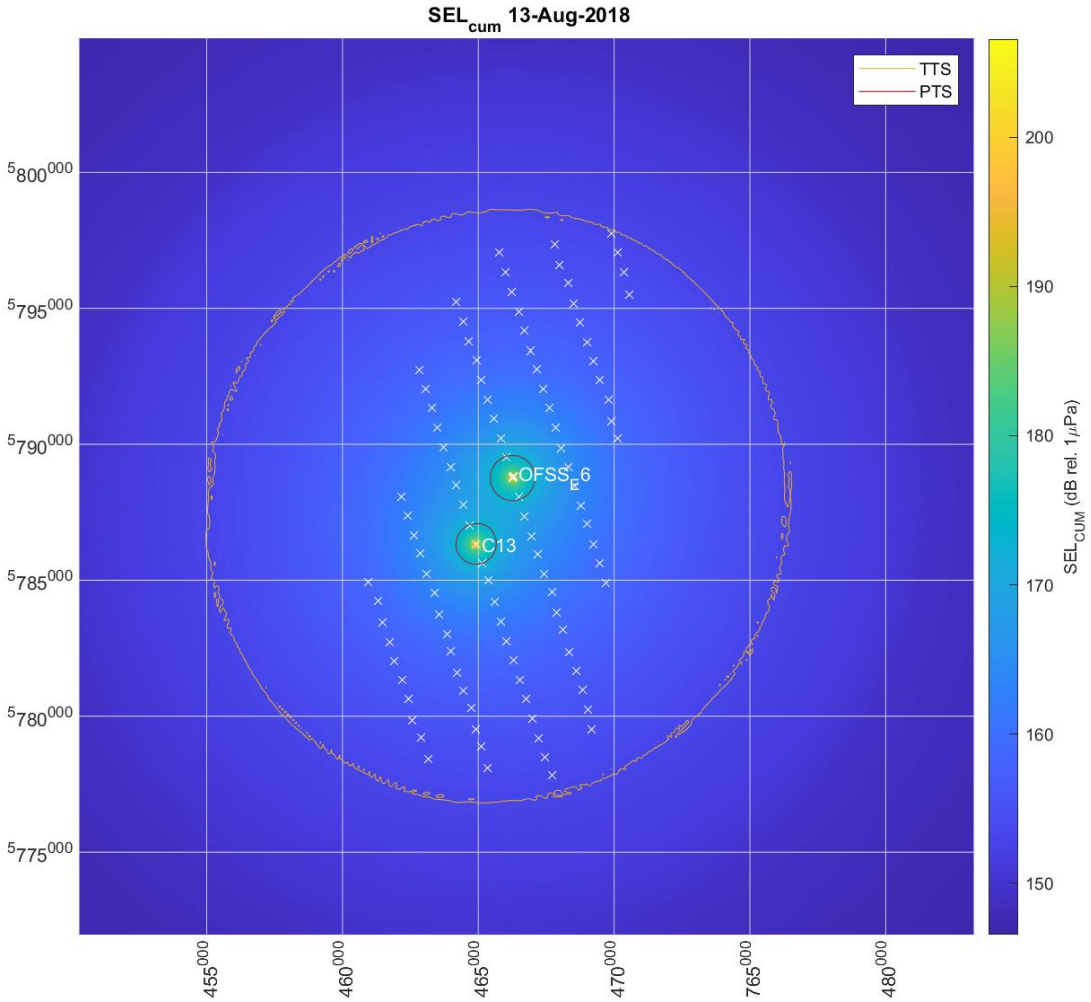

Figure 9 SEL_{CUM} for the calendar day 13^{sth} August 2020 when piling and ADD occurred at the OFSS substation and C13. SEL_{CUM} is calculated between 40 Hz and 16 kHz. Eastings and Northings are in meters.

	Range in meters			
	Piling Only		Piling + ADD	
	PTS	TTS	PTS	TTS
Maximum	820	8570	8080	8580
Minimum	100	740	100	740
Median	520	5190	600	5455

Table 5 Summary of results in table *Daily 24 hour SEL 07.xlsx*. The maximum, minimum and median range to the risk of PTS and TTS are shown for piling only and for piling combined with noise from ADD devices.

4. Discussion

The transmission loss profiles used to simulate underwater noise levels related to piling at the East Anglia One offshore wind farm, as well as present ADD noise were based on both the parabolic code RAMSGeo and a ray trace approach implemented in COMSOL Multiphysics. The RAMSGeo approach is very robust at low frequencies but is numerically inefficient at high frequencies, and would thus not be viable to model noise including the ADD at 16 kHz. Instead, at high frequencies a ray trace approach was used to solve the models above 3 kHz. Switching between these two approaches is a standard methodology within underwater noise modelling community. A sensitivity analysis was conducted to determine whether the range to PTS and TTS was dependent on the frequency at which the model switched from RAMSGeo to ray trace; the variation was negligible when switching at frequencies between 2 and 5 kHz. The author assesses that the approach used is sufficient for the purposes of calculating the impact of piling and ADD on harbour porpoises.

5. References

Ainslie, M. A., & McColm, J. G. (1998). A simplified formula for viscous and chemical absorption in sea water. *Journal of the Acoustical Society of America* 103, 1671-1672.

LeBlanc, L. R., Mayer, L., Rufino, M., Schock, S. G., & King, J. (1992). Marine sediment classification using the chirp sonar. *Journal of the Acoustical Society of America* 91, 107-115.

Southall, B. L., Finneran, J. J., Reichmuth, C., Nachtigall, P. E., Ketten, D. R., Bowles, A. E., . . . Tyack, P. L. (2019). Marine Mammal Noise Exposure Criteria: Updated Scientific Recommendations for Residual Hearing Effects. *Aquatic Mammals* 45, 125-232.

Urick, R. (1983). *Principles of underwater noise.* New York: McGraw.

6. Appendix A: Bathymetric data

Bathymetric data files downloaded from Admiralty Marine Data Portal on 25/5/2020

https://datahub.admiralty.co.uk/portal/apps/sites/#/marine-data-portal

1987 HI354 Smiths Knoll to South Falls Sheet 3.csv
1987 HI354 Smiths Knoll to South Falls Sheet 4.csv
1987 HI354 Smiths Knoll to South Falls Sheet 5.csv
1987 HI354 Smiths Knoll to South Falls Sheet 6.csv
1987 HI354 Smiths Knoll to South Falls Sheet 7.csv
1988 HI412 North Sea Deep Water Route Sheet 2.csv
1993 HI603 Eastern Gas Fields to Noord Hinder TSS Blk1-2.csv
1994 HI616 Smiths Knoll to Orford Ness Blk A007.csv
1994 HI616 Smiths Knoll to Orford Ness Blk A008.csv
1994 HI616 Smiths Knoll to Orford Ness Blk A009.csv
1994 HI616 Smiths Knoll to Orford Ness Blk A010.csv
1994 HI616 Smiths Knoll to Orford Ness Blk A011.csv
1994 HI616 Smiths Knoll to Orford Ness Blk A012.csv
1994 HI616 Smiths Knoll to Orford Ness Blk A013.csv
1994 HI616 Smiths Knoll to Orford Ness Blk A014.csv
1994 HI616 Smiths Knoll to Orford Ness Blk A015.csv
1994 HI616 Smiths Knoll to Orford Ness Blk A016.csv
1994 HI616 Smiths Knoll to Orford Ness Blk A017.csv
1994 HI616 Smiths Knoll to Orford Ness Blk A018.csv
1994 HI616 Smiths Knoll to Orford Ness Blk A019.csv
1994 HI616 Smiths Knoll to Orford Ness Blk A020.csv
1995 HI667 Orfordness to North Foreland Blk1.csv
1995 HI667 Orfordness to North Foreland Blk2.csv
1995 HI667 Orfordness to North Foreland Blk3.csv
1995 HI667 Orfordness to North Foreland Blk4.csv
1995 HI667 Orfordness to North Foreland Blk5.csv
1995 HI667 Orfordness to North Foreland Blk6.csv
1995 HI667 Orfordness to North Foreland Blk8.csv
1995 HI673 Brown Ridge TSS to North Hinder TSS Blk1.csv
1995 HI673 Brown Ridge TSS to North Hinder TSS Blk2.csv
1995 HI673 Brown Ridge TSS to North Hinder TSS Blk3.csv
1995 HI674 Smiths Knoll to Sandettie.csv
2000 HI910 North Sea Deep Water Blk1.csv
2000 HI910 North Sea Deep Water Blk2.csv
2001 HI922 South West TSS Blk1.csv
2001 HI922 South West TSS Blk2.csv
2001 HI922 South West TSS Blk3.csv